

# Ultrafast Long-Distance Electron-Hole Plasma Expansion in GaAs Mediated by Stimulated Emission and Reabsorption of Photons

Tinkara Troha,<sup>1</sup> Filip Klimovič<sup>2</sup>, Tomáš Ostatnický<sup>2</sup>, Filip Kadlec<sup>1</sup>, Petr Kužel,<sup>1</sup> and Hynek Němec<sup>1,\*</sup>

<sup>1</sup>*Institute of Physics ASCR, Na Slovance 2, 182 00 Prague 8, Czech Republic*

<sup>2</sup>*Charles University, Faculty of Mathematics and Physics, Ke Karlovu 3, 121 16 Prague 2, Czech Republic*

 (Received 23 June 2022; revised 13 March 2023; accepted 3 May 2023; published 31 May 2023)

Electron-hole plasma expansion with velocities exceeding  $c/50$  and lasting over 10 ps at 300 K was evidenced by time-resolved terahertz spectroscopy. This regime, in which the carriers are driven over  $> 30 \mu\text{m}$  is governed by stimulated emission due to low-energy electron-hole pair recombination and reabsorption of the emitted photons outside the plasma volume. At low temperatures a speed of  $c/10$  was observed in the regime where the excitation pulse spectrally overlaps with emitted photons, leading to strong coherent light-matter interaction and optical soliton propagation effects.

DOI: [10.1103/PhysRevLett.130.226301](https://doi.org/10.1103/PhysRevLett.130.226301)

Propagation speed of electrons in a crystal is a crucial parameter that determines the bandwidth of many electronic devices. Unlike in vacuum where the only limit is the speed of light  $c$ , electron velocity  $v_g = (1/\hbar)(\partial E/\partial k)$  in crystals is controlled by their electronic band structure. The slope of the dispersion  $E(k)$  is limited by the interaction of electron orbitals forming the conduction band and by its periodicity in the  $k$  space, implying that maximum electron transport velocity (for any kind of transport including the ballistic one) does not exceed a few times  $10^6 \text{ m/s} \approx c/100$  in known crystals.

The spatiotemporal dynamics of photoexcited electron-hole plasma (EHP) in semiconductors have attracted attention for decades as they frequently reveal velocities exceeding the ambipolar diffusion [1]. Depending on the excitation conditions, several phenomena have been identified, including Fermi pressure [2–4], thermodiffusive transport [5], screening of electron-phonon interaction [6], and stimulated emission recombination and reabsorption [7,8]. As anticipated, the observed expansion rates have not exceeded the above limit imposed by the band structure.

Here, we demonstrate that stimulated emission and subsequent reabsorption of low-energy photons in degenerate EHP can dramatically enhance plasma expansion rates, resulting in effective velocities exceeding  $c/50$  at room temperature. Free electrons and holes thus reappear together in the originally unexcited parts deep in the GaAs wafer, which may be effectively viewed as an ambipolar charge transport. Similar interconnection between electronic and photonic aspects proved recently useful in organic perovskite solar cells [9] but it may be also a factor for fast photoconductive semiconductor switches. Below 100 K, the EHP surface shifts at much higher velocity  $\sim c/10$ , reflecting propagation of an optical soliton in the highly excited semiconductor.

In our experiment, dense EHP was created by absorption of a short intense optical pulse with photon energy slightly above the band gap. The photon fluence was high enough to cause absorption saturation due to the filling of states (the absorption length  $l_0$  is thus considerably longer than the linear absorption depth), and to activate also the two-photon absorption [10]. The photoexcited area ( $\varnothing \geq 2 \text{ mm}$ ) was fundamentally larger than the photoexcited depth to reduce possible edge effects. The EHP thickness was then probed by a delayed THz pulse, taking advantage of the high reflectivity of metalliclike EHP surface for long-wavelength radiation. The employed “time-of-flight” method [10,11] uses counterpropagating optical pump and THz probe pulses separated by a controlled time delay  $t$ . The time required by the probe to pass from the back surface of a 0.7 mm thick (100)-GaAs, reflect on the EHP, and propagate to the back surface again is measured: the temporal shift  $\Delta\theta(t)$  of the output terahertz pulse represents plasma expansion by a distance  $c\Delta\theta(t)/(2\eta_{\text{THz}})$  ( $\eta_{\text{THz}} = 3.6$  is the terahertz refractive index of GaAs [12]). Experiments were performed with two different femtosecond systems: multipass amplifier Quantronix ODIN (800 nm, 1 kHz rep. rate, 55 fs pulse length) and regenerative amplifier Spitfire ACE (800 nm, 5 kHz, 40 fs). For more details on the methods, see Secs. S1 and S2 in [13].

The expansion dynamics of the EHP layer observed at room temperature [Fig. 1(a)] reveal an initial short delay ( $\sim 1 \text{ ps}$ ) independent of the excitation fluence, followed by a fast onset of EHP expansion, thus indicating that the EHP initial state is static, rather than having nonzero kinetic energy like in Refs. [29,30]. The expansion rate reaches its maximum shortly after the very beginning of the system evolution and then it monotonically slows down. The prominent effect is then the strong dependence of the initial velocity and the expansion distance on the excitation

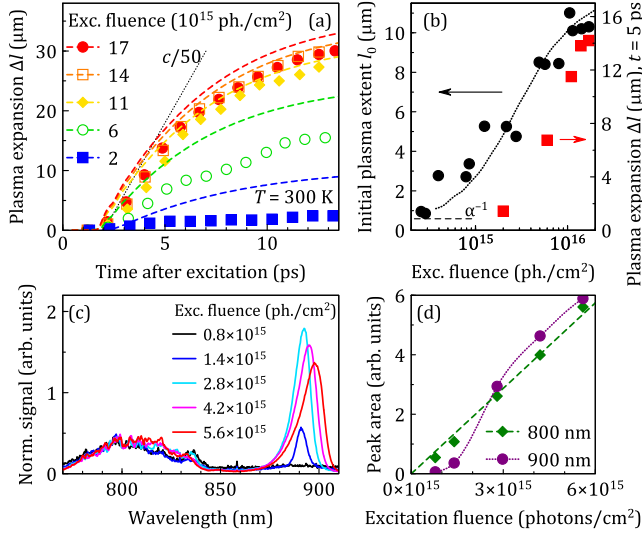


FIG. 1. (a) Increase in the plasma extent during the plasma expansion at room temperature. Symbols: measurements (using ODIN). Dashed lines: calculations (same parameters as in Fig. 3). Dotted line: slope corresponding to expansion velocity  $c/50$ . Zero time and plasma expansion distance are chosen such that the dynamics right after the full absorption of the excitation pulse is shown (see Secs. S1 and S2 of [13] for more details). (b) Comparison of the initial EHP extent  $l_0$  and EHP expansion  $\Delta l(5 \text{ ps}) = l(5 \text{ ps}) - l_0$ , which can serve as a measure of the initial EHP expansion rate. (c) Optical spectrum (normalized by the excitation fluence) measured behind a  $10 \mu\text{m}$  thick GaAs (Spitfire ACE) and (d) corresponding integrated areas of the broad peak around 800 nm and of that close to 900 nm in (c).

fluence and thus on the initial EHP thickness  $l_0$ . The effect saturates upon the pump fluence of  $\sim 10^{16}$  photons/cm<sup>2</sup>. We show in Fig. 1(b) that the plasma expansion distance  $\Delta l$  measured at a fixed time after photoexcitation correlates with the initial thickness  $l_0$  of the EHP [10] measured in the same experiment.

The most significant observation is the high EHP expansion velocity deduced from Fig. 1(a): it reaches  $c/50$ , thus exceeding the limit permitted by the band structure. The observed expansion distances are also strikingly long, not only compared with the electron mean free path in GaAs at room temperature ( $\sim 100 \text{ nm}$ ) but even

with the electron mean free path in high-quality GaAs 2D electron gas at low temperatures ( $\lesssim 10 \mu\text{m}$ , [31]). Although distances reaching  $250 \mu\text{m}$  were reported in [2], that effect was observed only at very low temperatures (2 K) and attributed to a slow motion of neutral excitons (velocity  $\sim c/3000$ ).

We interpret the observed ultrafast EHP kinetics in terms of the photon-mediated transport of electron-hole pairs. Single-photon absorption of the incident pulse causes excitation of hot electron-hole pairs: the electrons have an initial excess energy according to the bandwidth of the pump pulse (average excess energy  $\Delta E \sim 130 \text{ meV}$ ) [Figs. 2(a) and 2(b)]. Within a few hundreds of femtoseconds [32,33], an electron-electron interaction drives the charges to a thermal distribution and they start to cool down via phonon emission [Figs. 2(a) and 2(c)]. For high-enough excitation fluence, the thermalized EHP is degenerate. The medium thus becomes an efficient luminescent source and an optical amplifier for photons with energies lower than the difference between the Fermi energies of electrons and holes [Fig. 2(d)]. The emission is amplified in the area with degenerate EHP and it is then reabsorbed deeper in the sample where unoccupied states are available [Fig. 2(d)], resulting in the spatial shift of the EHP surface.

The amplified emission was indeed observed behind a thin GaAs wafer [Figs. 1(c) and 1(d)]. The intensity of the excitation spectrum around 800 nm scales linearly with the excitation fluence: since there is no sudden transmission increase, we conclude that a part of the sample remains unbleached. The presence of the threshold for the long-wavelength emission then confirms that its origin is a stimulated emission. The red shift stems from band-gap narrowing due to the increased temperature and carrier concentration.

The prerequisites for the ultrafast EHP expansion are thus (i) existence of a degenerate EHP through which lower-energy above-band-gap photons can freely propagate and can be amplified, and (ii) presence of a reservoir maintaining the degeneracy of the EHP. The flow of the lower-energy photons—and in turn, also the EHP expansion rate—should thus be proportional to the initial thickness  $l_0$  of EHP, which is controlled by the excitation fluence. As already discussed, Fig. 1(b) shows the

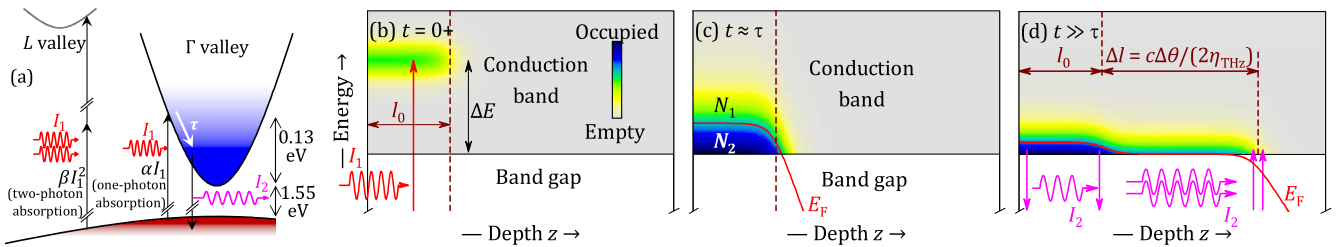


FIG. 2. (a) Illustration of processes occurring in the band structure of GaAs; see also Sec. S5 in [13]. (b)–(d) Schematics of the evolution of the carrier distribution in the real space: (b) immediately after photoexcitation, (c) after carrier cooling, and (d) during the plasma expansion regime.

correlation between the EHP expansion rate and  $l_0$  with the same saturation threshold of  $\sim 10^{16}$  photons/cm<sup>2</sup>. Above this critical value, both the plasma expansion rate and distance are almost constant. This behavior is directly linked to the initial linear increase in  $l_0$  with excitation fluence and its saturation due to two-photon absorption for high fluences [10]. Although the two-photon absorption generates additional electron-hole pairs in the  $L$  valley, the relaxation of holes to the  $\Gamma$  valley requires a cascade of scattering events with low- $k$  phonons lasting several picoseconds. Thus,  $L$ -valley charges cannot significantly contribute to the stimulated emission during the observation window.

Quantitative insight into the EHP dynamics is obtained from a simple model considering two discrete energy levels for electrons involving the states above (reservoir, level 1) and below (active level 2) the initial Fermi level. The respective numbers of available states per unit volume  $N_1$  and  $N_2$  are calculated from the band structure of GaAs:  $N_1$  is the number of states accessible within the bandwidth of the pump pulse [10];  $N_2$  is taken as the initial number of states per unit volume below the Fermi level at the front surface. Propagation in one dimension is considered since the lateral size of EHP exceeds its thickness  $> 50\times$ .

The population densities  $n_1(z, t)$  and  $n_2(z, t)$  in levels 1 and 2, respectively, follow simple rate equations (Sec. S6 of [13]):

$$\frac{\partial n_1}{\partial t} = \frac{\alpha}{\hbar\omega_1} \left[ 1 - \frac{2n_1}{N_1} \right] I_1 - \frac{1}{\tau} \left[ 1 - \frac{n_2}{N_2} \right] n_1 \quad (1)$$

$$\frac{\partial n_2}{\partial t} = \frac{\alpha}{\hbar\omega_2} \left[ 1 - \frac{2n_2}{N_2} \right] I_2 + \frac{1}{\tau} \left[ 1 - \frac{n_2}{N_2} \right] n_1 - An_2. \quad (2)$$

Each level is associated with its own photon field: charges in the reservoir are generated by the excitation pulse with frequency  $\omega_1$  and optical power density  $I_1(z, t)$ , whereas the stimulated emission and reabsorption of charges in the active level is represented by the fields with a lower photon frequency,  $\omega_2$ , and power densities  $I_2^\pm(z, t)$  (the superscripts + and - denote the radiation propagating forward and backward, respectively;  $I_2 \equiv I_2^+ + I_2^-$ ). The propagation of photons is governed by the equations:

$$\frac{1}{v} \frac{\partial I_1}{\partial t} + \frac{\partial I_1}{\partial z} = -\alpha \left[ 1 - \frac{2n_1}{N_1} \right] I_1 - \beta I_1^2 \quad (3)$$

$$\frac{1}{v} \frac{\partial I_2^\pm}{\partial t} \pm \frac{\partial I_2^\pm}{\partial z} = -\alpha \left[ 1 - \frac{2n_2}{N_2} \right] I_2^\pm + \frac{1}{2} A \hbar\omega_2 n_2, \quad (4)$$

where  $v$  is the group velocity of the excitation pulse in GaAs near the band-gap edge. The first right-hand-side (rhs) terms of Eqs. (1)–(4) describe the absorption or stimulated emission ( $\alpha$  is the linear absorption coefficient). The second rhs terms in Eqs. (1) and (2) stand for the

relaxation of charges (with characteristic time  $\tau$ ) from the reservoir to the active level including its saturation. The term  $-\beta I_1^2$  in Eq. (3) describes the depletion of the excitation field by two-photon absorption. The spontaneous emission [rate  $A$  in Eqs. (2) and (4)] is important only for the active level, where it can be amplified.

The factors 1/2 in Eq. (4) account for effective renormalization of the group velocity of re-emitted photons due to the directional dispersion of their wave vectors in 3D. In the calculations, 80% of the backward propagating radiation  $I_2^-$  is reflected back at the front GaAs surface, thus being transformed into the  $I_2^+$  intensity (the value represents the internal reflectivity averaged over angles of incidence and polarization).

The resulting dynamics at high excitation fluences are illustrated in Fig. 3 and the results are also directly compared with the experimental data in Fig. 1(a). The pump pulse generates charge carriers deep in GaAs [ $l_0 \sim 15 \mu\text{m}$ , Fig. 3(a)] due to saturation of absorption [10]. These charges then need a time comparable with  $\tau$  to relax to the active level and create a population inversion [ $t \sim 1$  ps, Fig. 3(b)]. An extra time is needed for the spontaneous emission to develop and to initiate the stimulated emission [ $t \sim 1.5$  ps, Fig. 3(c)], producing a burst of photons that can be reabsorbed only deep in the bulk in the nonexcited areas of GaAs; this reabsorption is responsible for the plasma expansion observed experimentally. Note that a comparable delay between the photoexcitation and the onset of the plasma expansion was indeed observed experimentally [Fig. 1(a)].

Just after the initial carrier relaxation, when a quasi-equilibrium between the reservoir and the active level is reached, the total outflow of re-emitted photons can be analytically estimated from Eqs. (1)–(4), leading to the early-time plasma expansion velocity (see Sec. S7 in [13]):

$$u_{\text{max}} = \frac{l_0}{2\tau} \frac{N_1 - N_2}{N_2}. \quad (5)$$

This formula permits one to fully understand the saturation mechanisms in Figs. 1(a) and 1(b). The expansion rate is proportional to the number of available charges above the Fermi level,  $l_0(N_1 - N_2)/2$ . This confirms that the key parameter is indeed the initial EHP thickness  $l_0$ . Ziebold *et al.* conducted a similar experiment and observed an EHP expansion velocity in GaAs  $\sim 10^4$  m/s, much lower compared to our results [4]. In their work, the excess energy was much higher (several hundred meV above the band gap), implying a submicron absorption length independent of the excitation fluence. In agreement with Eq. (5), the fast expansion mediated by stimulated emission and reabsorption thus could not develop.

To further investigate the expansion of the degenerate EHP, we conducted experiments at lower temperatures while keeping the energy of excitation photons unchanged.

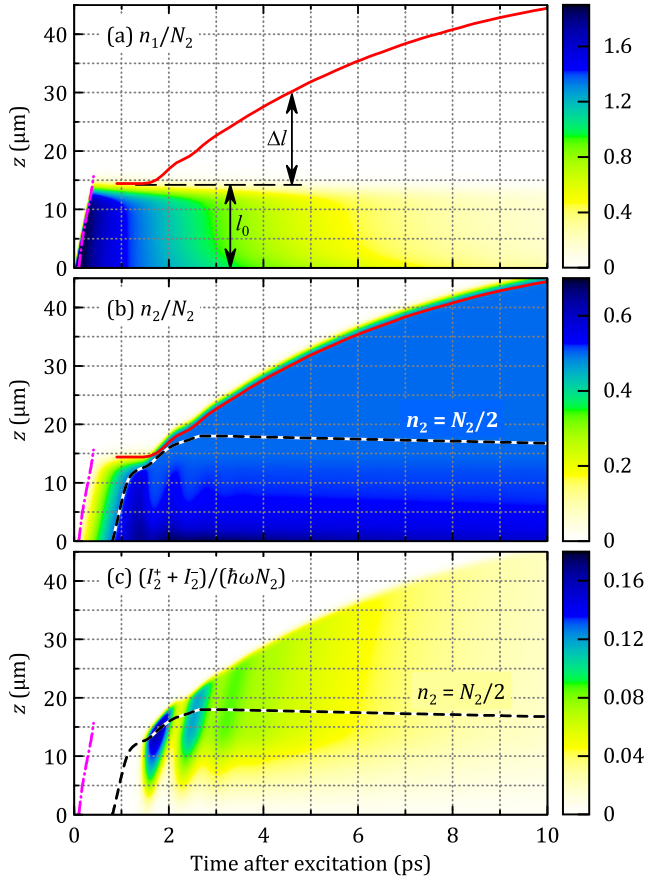


FIG. 3. Calculated dynamics of (a) the populations  $n_1$  and (b)  $n_2$ , and (c) of the optical power density  $I_2$ . The magenta dash-dot line indicates the propagation of the peak of the excitation pulse  $I_1$  (the deviations from the straight light line are caused by the pulse reshaping due to the nonlinear interaction with the reservoir). The dashed curve in (b) and (c) divides the region into areas below and above the population inversion threshold in the active level. The red solid curve shows the position where the terahertz pulse appears to be reflected (result of numerical calculations of terahertz beam propagation in the displayed gradient environment with carrier density  $n_1 + n_2$ ; see Sec. S3 in [13]). Parameters: incident excitation fluence  $= 1.9 \times 10^{16}$  photons/cm<sup>2</sup>,  $N_2 = 1.34 \times 10^{18}$  cm<sup>-3</sup>,  $\tau = 2$  ps (estimate based on [34–36]),  $N_1 = 5 \times 10^{18}$  cm<sup>-3</sup> [10],  $\alpha = 1.3 \mu\text{m}^{-1}$  [37],  $v = c/4.2$  [37],  $\beta = 220$  cm/GW [10],  $A = 1$  ns<sup>-1</sup> [38], excitation pulse length = 100 fs. The material parameters correspond to room temperature properties of GaAs. See Sec. S2 of [13] for the meaning of “time after excitation”.

The cooling decreased the initial excess energy down to 77 meV (180 K), 49 meV (100 K), or 32 meV (20 K) as a result of the band-gap renormalization (note that the FWHM of the pump pulse spectrum is  $\sim 60$  meV). The resulting plasma expansion dynamics and the extracted velocities are shown in Fig. 4. Since  $l_0$  is longer, we observe the expected increase in the expansion velocity above  $c/40$  at 180 K, further above the limit provided by the band structure. Upon decreasing the temperature to

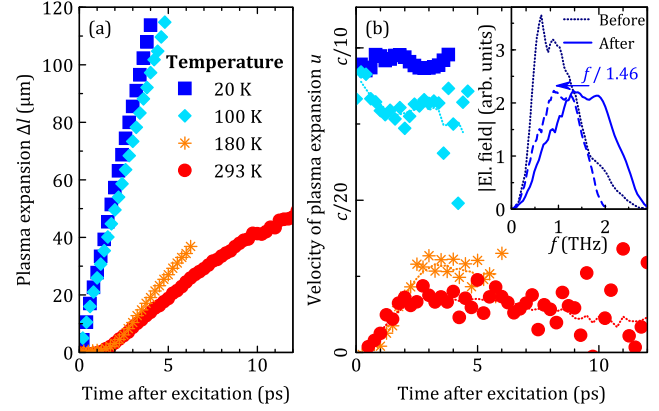


FIG. 4. Temperature dependence of (a) increase in plasma extent during its expansion and (b) velocity of plasma expansion at the excitation fluence  $1.7 \times 10^{16}$  photons/cm<sup>2</sup>. The lines in (b) are just smoothed data to guide the eye. Inset: amplitude of the spectrum of the detected THz pulse before and after photoexcitation of the front side, measured at  $T = 20$  K. The observed blue shift corresponds to the Doppler factor  $\sqrt{(c/\eta_{\text{THz}} + u)/(c/\eta_{\text{THz}} - u)} \approx 1.46$  and it therefore independently confirms that the velocity of the plasma expansion  $u$  is  $\approx c/10$ . Experiments with Spitfire ACE.

100 K and below, we observed even faster propagation of the EHP surface:  $c/13$  (100 K) and  $\sim c/10$  (20 K). The high observed velocities were independently quantitatively confirmed by an observed Doppler shift [inset of Fig. 4(b)]. Since the recorded high-speed propagation spans over several picoseconds (much longer than the THz pulse duration), both time of flight and Doppler shift provide reliable results free of possible transition effects.

The time dependence at low temperatures [Fig. 4(a)] qualitatively differs from those observed at  $\geq 180$  K: the motionless phase due to carrier cooling is missing and the propagation velocity does not decrease with time. The immediate motion and high velocity indicate that the apparent plasma expansion at low temperatures in fact represents propagation of the excitation pulse. The long propagation distance ( $> 100 \mu\text{m}$ ) and small velocity compared to the linear group velocity ( $\approx c/4.2$  [37]) rule out the possibility that the observed effect is caused by the group velocity dispersion and excitation pulse reshaping due to absorption. We interpret these effects in terms of coherent electron-photon interaction that leads to optical soliton propagation and self-induced transparency [39,40]. Prerequisites for these phenomena are met in our system [41,42], namely large pulse area and sufficiently slow dephasing close to the band gap at low temperature [43–45]. Theoretical estimation [39,40] predicts propagation velocity  $c/10.5$  for 40 fs pulses at 20 K, in accord with the experimental observation (see also Sec. S4 in [13]).

We stress that large expansion distances and velocities were observed with two laser systems with different amplification principles, which confirms that the large

observed expansion rate is an inherent characteristic of the EHP itself. The small differences between the dynamics under comparable conditions stem from different spatial profiles of the excitation pulses.

In summary, we found that an intense above-gap photoexcitation of GaAs may create population inversion conditions for photons with energies slightly above the band gap. The emission together with the reabsorption of the emitted photons efficiently mediates a long-lasting ( $> 10$  ps) ultrafast expansion of the degenerate electron-hole plasma with velocities reaching  $c/50$  at room temperature. The developed two-level model is sufficient to describe the observed dynamics, with only a few roughly estimated parameters (e.g., uncertainties in  $\tau$  exist in the literature [34–36]). The results suggest that the ultrafast plasma expansion should be present in most direct-gap semiconductors when a thick layer of degenerate EHP is created. At lower temperatures, wider band gap and less pronounced electron dephasing allowed us to observe propagation of optical soliton over  $> 100 \mu\text{m}$  at velocity  $\sim c/10$  in a good agreement with theoretical predictions.

We acknowledge fruitful discussions with Karel Výborný, who substantially helped us to decode the nature of the observed phenomenon. We also acknowledge the financial support by the Czech Science Foundation (Project No. 23-05640S), and Charles University grant (SVV-2023-260720).

---

\*Corresponding author.  
nemecek@fzu.cz

- [1] F. A. Majumder, H.-E. Swoboda, K. Kempf, and C. Klingshirn, *Phys. Rev. B* **32**, 2407 (1985).
- [2] K. M. Romanek, H. Nather, J. Fischer, and E. O. Göbel, *J. Lumin.* **24–25**, 585 (1981).
- [3] A. Cornet, M. Pugnet, J. Collet, T. Amand, and M. Brousseau, *J. Phys. (Paris), Colloq.* **42**, 471 (1981).
- [4] R. Zibold, T. Witte, M. Hübner, and R. G. Ulbrich, *Phys. Rev. B* **61**, 16610 (2000).
- [5] K. T. Tsen and H. Morkoc, *Phys. Rev. B* **34**, 6018 (1986).
- [6] M. R. Junnarkar and R. R. Alfano, *Phys. Rev. B* **34**, 7045 (1986).
- [7] E. C. Fox and H. M. van Driel, *Phys. Rev. B* **47**, 1663 (1993).
- [8] I. J. Blewett, N. R. Gallaher, A. K. Kar, and B. S. Wherrett, *J. Opt. Soc. Am. B* **13**, 779 (1996).
- [9] S. G. Motti, T. Crothers, R. Yang, Y. Cao, R. Li, M. B. Johnston, J. Wang, and L. M. Herz, *Nano Lett.* **19**, 3953 (2019).
- [10] F. Kadlec, H. Němec, and P. Kužel, *Phys. Rev. B* **70**, 125205 (2004).
- [11] D. M. Mittleman, S. Hunsche, L. Boivin, and M. C. Nuss, *Opt. Lett.* **22**, 904 (1997).
- [12] D. Grischkowsky, S. Keiding, M. van Exter, and C. Fattinger, *J. Opt. Soc. Am. B* **7**, 2006 (1990).
- [13] See Supplemental Material, which includes Refs. [14–28], at <http://link.aps.org/supplemental/10.1103/PhysRevLett.130.226301> for additional details.
- [14] R. Jacobsson, in *Progress in Optics*, edited by E. Wolf (North-Holland, Amsterdam, 1965), Chap. 5, pp. 255–258.
- [15] T. E. Ostromek, *Phys. Rev. B* **54**, 14467 (1996).
- [16] F. Sekiguchi, T. Mochizuki, C. Kim, H. Akiyama, L. N. Pfeiffer, K. W. West, and R. Shimano, *Phys. Rev. Lett.* **118**, 067401 (2017).
- [17] H. Haug and S. W. Koch, *Quantum Theory of the Optical and Electronic Properties of Semiconductors*, 4th ed. (World Scientific, Singapore, 2005).
- [18] H. Giessen, S. Linden, J. Kuhl, A. Knorr, S. W. Koch, M. Hetterich, M. Grün, and C. Klingshirn, *Opt. Express* **4**, 121 (1999).
- [19] H. Giessen, A. Knorr, S. Haas, S. W. Koch, S. Linden, J. Kuhl, M. Hetterich, M. Grün, and C. Klingshirn, *Phys. Rev. Lett.* **81**, 4260 (1998).
- [20] N. C. Nielsen, S. Linden, J. Kuhl, J. Förstner, A. Knorr, S. W. Koch, and H. Giessen, *Phys. Rev. B* **64**, 245202 (2001).
- [21] C. Fürst, A. Leitenstorfer, A. Nutsch, G. Tränkle, and A. Zrenner, *Phys. Status Solidi (b)* **204**, 20 (1997).
- [22] A. Schülzgen, R. Binder, M. E. Donovan, M. Lindberg, K. Wundke, H. M. Gibbs, G. Khitrova, and N. Peyghambarian, *Phys. Rev. Lett.* **82**, 2346 (1999).
- [23] M. D. Sturge, *Phys. Rev.* **127**, 768 (1962).
- [24] R. K. Bullough, P. J. Caudrey, J. D. Gibbon, and S. Duckworth, *Opt. Commun.* **18**, 200 (1976).
- [25] M. L. Cohen and J. R. Chelikowsky, *Electronic Structure and Optical Properties of Semiconductors*, Springer Series Solid-State Science Vol. 75 (Springer, Berlin, Heidelberg, 1988), p. 103.
- [26] J. S. Blakemore, *J. Appl. Phys.* **53**, R123 (1982).
- [27] J. F. Young and H. M. van Driel, *Phys. Rev. B* **26**, 2147 (1982).
- [28] D. J. Griffiths, *Introduction to Quantum Mechanics* (Prentice Hall, Englewood Cliffs, 1995), p. 197.
- [29] M. D. Thomson, S. M. Tzanova, and H. G. Roskos, *Phys. Rev. B* **87**, 085203 (2013).
- [30] N. Kohno, R. Itakura, and M. Tsubouchi, *Phys. Rev. B* **102**, 235201 (2020).
- [31] C. W. J. Beenakker and H. van Houten, *Solid State Phys.* **44**, 1 (1991).
- [32] L. Rota, P. Lugli, T. Elsaesser, and J. Shah, *Phys. Rev. B* **47**, 4226 (1993).
- [33] H. Tanimura, K. Tanimura, and J. Kanasaki, *Phys. Rev. B* **104**, 245201 (2021).
- [34] S. S. Prabhu and A. S. Vengurlekar, *J. Appl. Phys.* **95**, 7803 (2004).
- [35] J. P. Callan, A. M.-T. Kim, L. Huang, and E. Mazur, *Chem. Phys.* **251**, 167 (2000).
- [36] A. Othonos, *J. Appl. Phys.* **83**, 1789 (1998).
- [37] D. E. Aspnes and A. A. Studna, *Phys. Rev. B* **27**, 985 (1983).
- [38] P. D. Dapkus, N. Holonyak, R. D. Burnham, D. L. Keune, J. W. Burd, K. L. Lawley, and R. E. Walline, *J. Appl. Phys.* **41**, 4194 (1970).
- [39] L. Allen and J. H. Eberly, *Optical Resonance and Two-Level Atoms* (John Wiley and Sons, New York, 1975).
- [40] S. L. McCall and E. L. Hahn, *Phys. Rev.* **183**, 457 (1969).

- [41] Th. Östreich and A. Knorr, *Phys. Rev. B* **48**, 17811 (1993).
- [42] S. W. Koch, A. Knorr, R. Binder, and M. Lindberg, *Phys. Status Solidi B* **173**, 177 (1992).
- [43] M. Joschko, M. Woerner, T. Elsaesser, E. Binder, T. Kuhn, R. Hey, H. Kostial, and K. Ploog, *Phys. Rev. Lett.* **78**, 737 (1997).
- [44] M. Joschko, M. Hasselbeck, M. Woerner, T. Elsaesser, R. Hey, H. Kostial, and K. Ploog, *Phys. Rev. B* **58**, 10470 (1998).
- [45] L. Bányai, Q. T. Vu, B. Mieck, and H. Haug, *Phys. Rev. Lett.* **81**, 882 (1998).